

Supporting Information

Content:

1. Experimental: synthesis, spectroscopic and analytical characterization of the new compounds.
 2. Temperature-dependent 600 MHz ^1H NMR spectra of (*E/Z*)-**2** in CDCl_3 .
 3. a) Fluorescence spectra of **2** (10 μM) in CH_3CN with 1.equiv. of different zinc salts: $\text{Zn}(\text{acac})_2$, $\text{Zn}(\text{OAc})_2$, $\text{Zn}(\text{OTf})_2$, $\text{Zn}(\text{NO}_3)_2$, ZnSO_4 , and ZnCl_2 .
b) Fluorescence spectra of **2-ZnOAc** in MeOH , CHCl_3 , *n*-Hexane.
c) Fluorescence spectra of (*E/Z*)-**2** (10 μM) in acetonitrile/water mixture.
 4. ^1H NMR spectra (600 MHz) of (*E/Z*)-**2** (5 mM) upon titration with $\text{Zn}(\text{OAc})_2$ in CD_3CN .
 5. UV-VIS data:
 - a) Absorption spectra of **2** and **2-ZnOAc** in *n*-Hexane, CHCl_3 , MeOH .
 - b) Determining associating constant from UV-VIS titration
 6. Crystallographic data.
 7. Topological analyses.
- 1. Experimental: synthesis, spectroscopic and analytical characterization of new compounds.**

Materials and instrumentations

All of the solvents for the UV and fluorescence spectra were obtained from Sigma-Aldrich or Merck and were of spectroscopic purity. The solution of metal salts were prepared from ZnCl_2 , ZnSO_4 , $\text{Zn}(\text{NO}_3)_2$, $\text{Zn}(\text{OTf})_2$, $\text{Zn}(\text{acac})_2$, $\text{Zn}(\text{OAc})_2$, $\text{Cu}(\text{acac})_2$, $\text{Ni}(\text{acac})_2$, $\text{Co}(\text{acac})_2$, $\text{Cd}(\text{acac})_2$, $\text{Hg}(\text{OAc})_2$, NaOAc , $\text{Pb}(\text{OAc})_2$, $\text{Mg}(\text{OAc})_2$. Melting points were determined on a Boetius PHMK 05 melting point apparatus. IR spectra were measured on Thermo Scientific Nicolet IR200 FT-IR. The ^1H NMR and ^{13}C NMR spectra were recorded with Bruker Avance III 600 at 300 K. The chemical shifts (δ) are reported in parts per million (ppm) on a δ scale downfield from TMS. The ^1H NMR spectra were referenced internally to the residual proton resonance in CDCl_3 (δ 7.26 ppm), $\text{DMSO}-d_6$ (δ 2.49 ppm), and CD_3CN (δ 1.96 ppm). The ^{13}C NMR spectra were referenced to CDCl_3 (δ 77.0 ppm), or), $\text{DMSO}-d_6$ (δ 39.7 ppm). The coupling constants (J) are reported in Hertz (Hz). Mass spectra were measured on Finnigan Mat 95 (EI, 70 eV) and ESI spectrometers. Microanalyses were performed with Vario Micro Tube CHNS; the results agreed with the calculated values.

The absorption spectra for compound **2** and **2-ZnOAc** were recorded with a Microplate Reader Infinite M200 (Tekan) spectrophotometer in 1 cm cells at 25 °C.

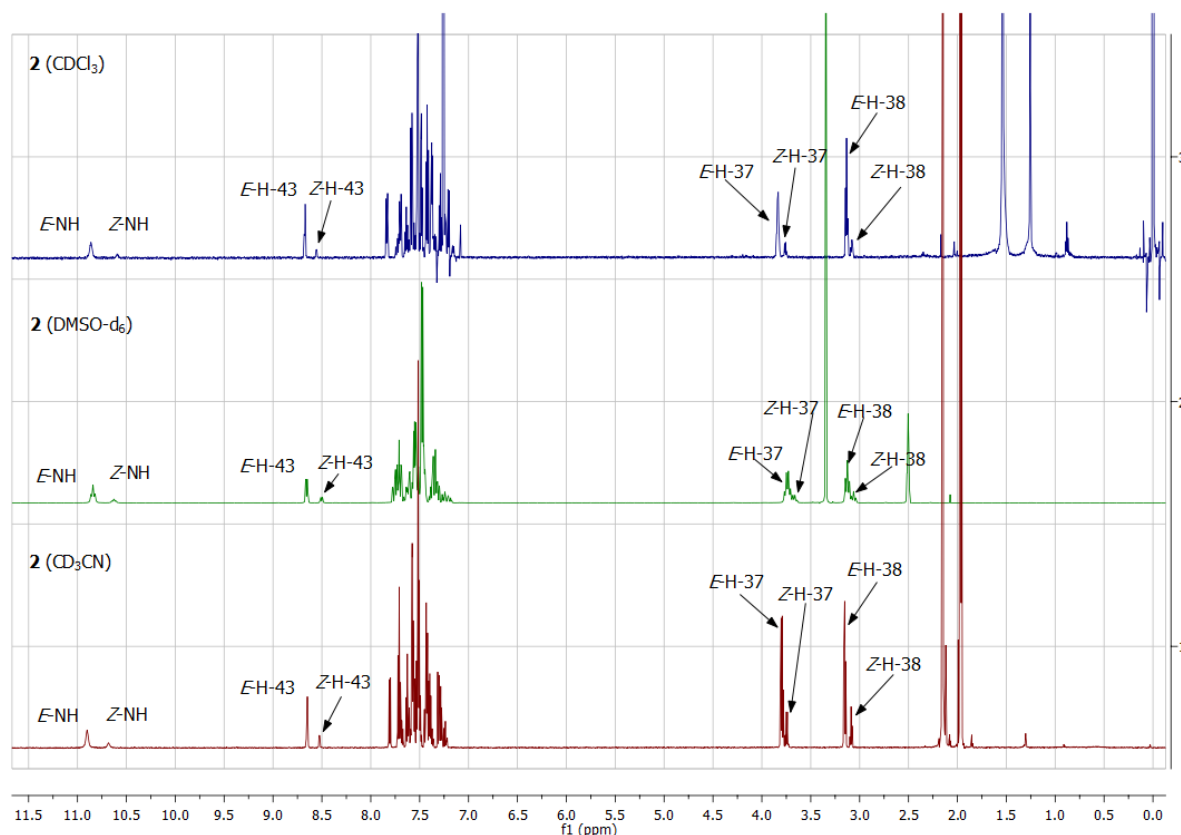
The fluorescence measurements for **2** and **2-ZnOAc** were obtained using a Hitachi F-4500 spectrofluorometer. All spectra were recorded at 25°C with an excitation slit width of 5 nm,

an emission slit of 5 nm and 400V (compare data in Fig. 4), 600 V (compare data for (*pR*)-**2**/*(pS*)-**2** and (*rac*)-**2** shown in Fig. 1) or 700V (compare data for suspension of **2** in CH₃CN/H₂O shown in Fig. 1) of PMT voltage.

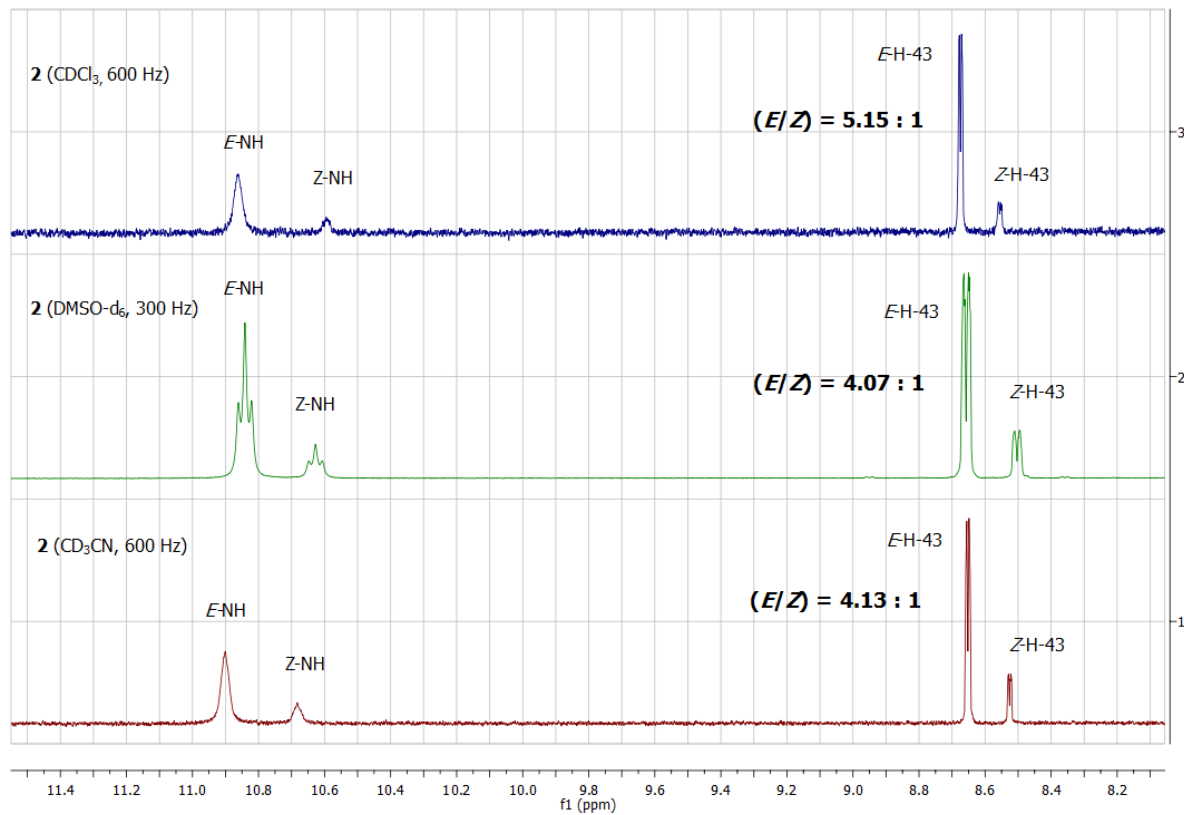
(E/Z)-3-[{2-(2-aminoethyl)pyridine]-phenylmethylidene}-1,4-dihydro-2*H*-1-phenylpyrrolo[2,3-*b*]quinoxalin-2-one **2:** 1-Aryl-1,4-dihydro-2*H*-3-thiobenzoylpyrrolo[2,3-*b*]quinoxalin-2-one **1** (0.5 g, 1.31 mmol) was added to the 2-(2-aminoethyl)pyridine (1.5 mL) in PrOH (5 mL). After 5 min, gas evolution (H₂S) was observed. The mixture was left for 2 hours, and then diluted with cold H₂O (100 mL). The precipitated solid was collected by filtration, washed with H₂O, and crystallised from acetonitrile. **2**: yellow needles, (0.59 g, 95.9%), m.p. 159 °C; (*E/Z*) = 5.15 : 1 (CDCl₃), (*E/Z*) = 4.13 : 1 (CD₃CN), (*E/Z*) = 4.07:1 (DMSO-*d*₆). IR (KBr): 3059, 2940, 2884, 1698, 1588, 1567 cm⁻¹. ¹H NMR (600 MHz, CD₃CN): δ 10.86 (s, 1H, *E*-NH), 10.65 (s, 1H, *Z*-NH), 8.62 (d, *J* = 4.8 Hz, 1H, *E*-H-43), 8.50 (d, *J* = 4.8 Hz, 1H, *Z*-H-43), 7.77 (dd, *J* = 7.56, 1.64 Hz, 1H, *E*-H-5), 7.89 – 7.19 (m, 33H, *E/Z*-Ar-H), 3.76 (q, *J* = 6.24 Hz, 2H, *E*-H-37), 3.71 (q, *J* = 6.24 Hz, 2H, *Z*-H-37), 3.12 (t, *J* = 6.48 Hz, 2H, *E*-H-38), 3.05 (t, *J* = 6.48 Hz, 2H, *Z*-H-38). ¹³C NMR (75.47 MHz, DMSO-*d*₆): δ = 37.64, 43.65, 89.73, 122.37, 123.91, 124.20, 126.52, 127.04, 127.28, 127.62, 127.78, 127.92, 128.11, 128.30, 128.45, 128.84, 129.01, 129.29, 130.22, 130.34, 131.18, 131.49, 134.01, 137.12, 137.21, 138.58, 138.94, 145.61, 146.74, 149.72, 158.30, 165.35. MS-ESI: m/z 470 (M⁺ +1). Anal. Calcd. for C₃₀H₂₃N₅O: C, 76.74; H, 4.94; N, 14.92. Found: C, 76.59; H, 4.83; N, 14.93.

Melting point: (*rac*)-**2**, 159 °C; (*pS*)-**2**/ (*pR*)-**2**, 170-171 °C.

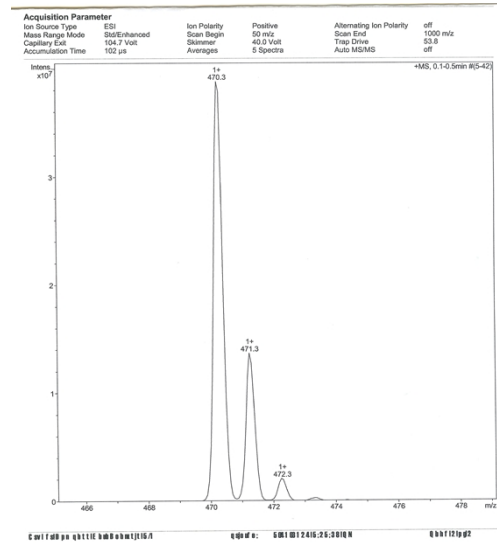
¹H NMR spectra of (*E/Z*)-**2** in CDCl₃, DMSO-*d*₆ and CD₃CN.



Partial ^1H NMR spectra of (*E/Z*)-2 in CDCl_3 , $\text{DMSO}-d_6$ and CD_3CN with the integral area for (*E/Z*)-H-43 diagnostic signals.



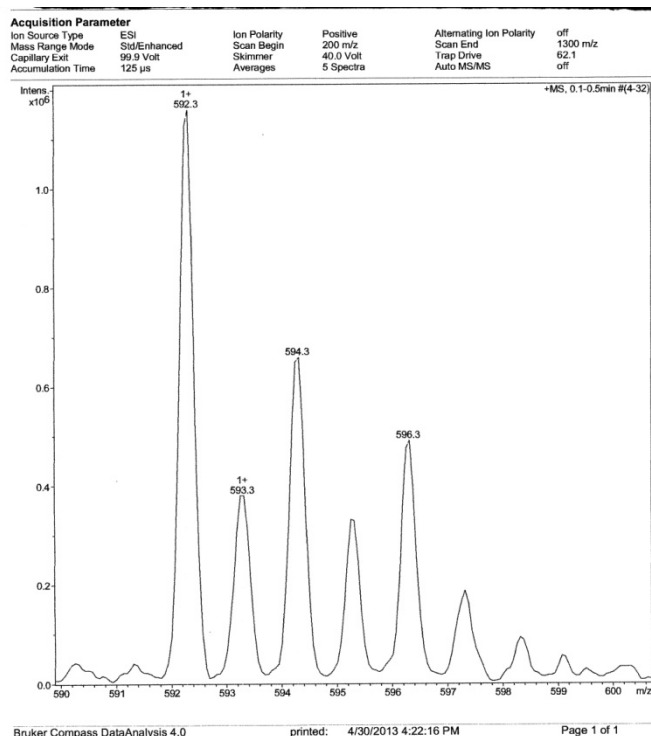
MS-ESI spectra for 2.



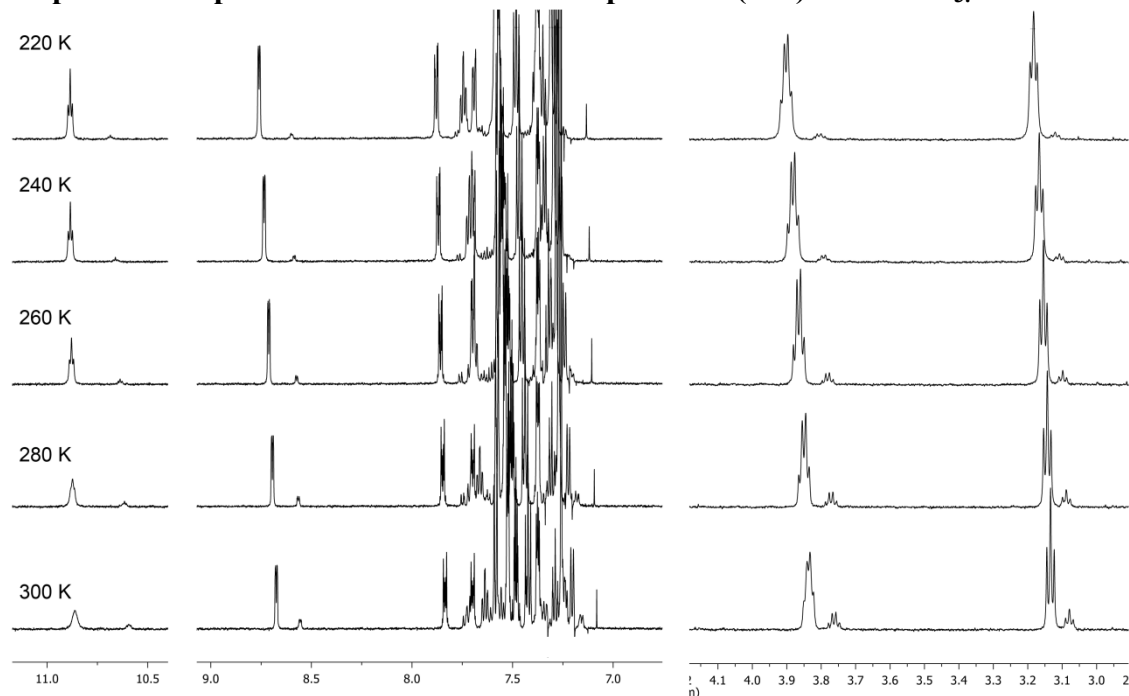
2-ZnOAc: To a solution of ligand **2** (112 mg 0.24 mmol) in anhydrous MeOH (3 mL) was added $\text{Zn}(\text{OAc})_2$ (44 mg, 0.24 mmol), and the mixture was refluxed for 5 hours. The reaction mixture was then allowed to cool to rt. The product precipitated from the reaction mixture as yellow powder, then was collected, washed with water, and crystallised from acetonitrile: light orange needles, (0.120 mg, 85.0%), m.p. 198-200 °C; IR (KBr): 3059, 3031, 2992,

2899, 2843, 1690, 1591, 1569, 1540 cm^{-1} . ^1H NMR (600.206 MHz, CD_3CN): δ 8.75 (d, $J = 5.3$, Hz, 1H, E-H-6'), 8.30 (d, $J = 8.3$ Hz, 1H, E-H-5), 8.04 (dt, $J = 7.8$ Hz, $J = 1.77$ Hz, 1H), 7.74 (d, $J = 8.3$ Hz, 1H), 7.72 (d, $J = 8.3$ Hz, 1H, Ar-H), 7.54 – 7.45 (m, 10H, Ar-H), 7.40 – 7.37 (m, 1H, Ar-H), 7.23 (d, $J = 8.3$ Hz, 2H, Ar-H), 3.63 (m, 2H, H- CH_2NH), 3.33 (m, 2H, CH_2NPy), 1.99 (s, 3H, CH_3COO^-). MS-ESI: m/z 592 (M^+). Anal. Calcd. for $(\text{LZnOAc})_2 \times (\text{H}_2\text{O} + \text{CH}_3\text{CN})$ $\text{C}_{66}\text{H}_{55}\text{N}_{11}\text{O}_7\text{Zn}_2$: C, 63.67; H, 4.45; N, 12.38. Found: C, 63.58; H, 4.37; N, 12.78.

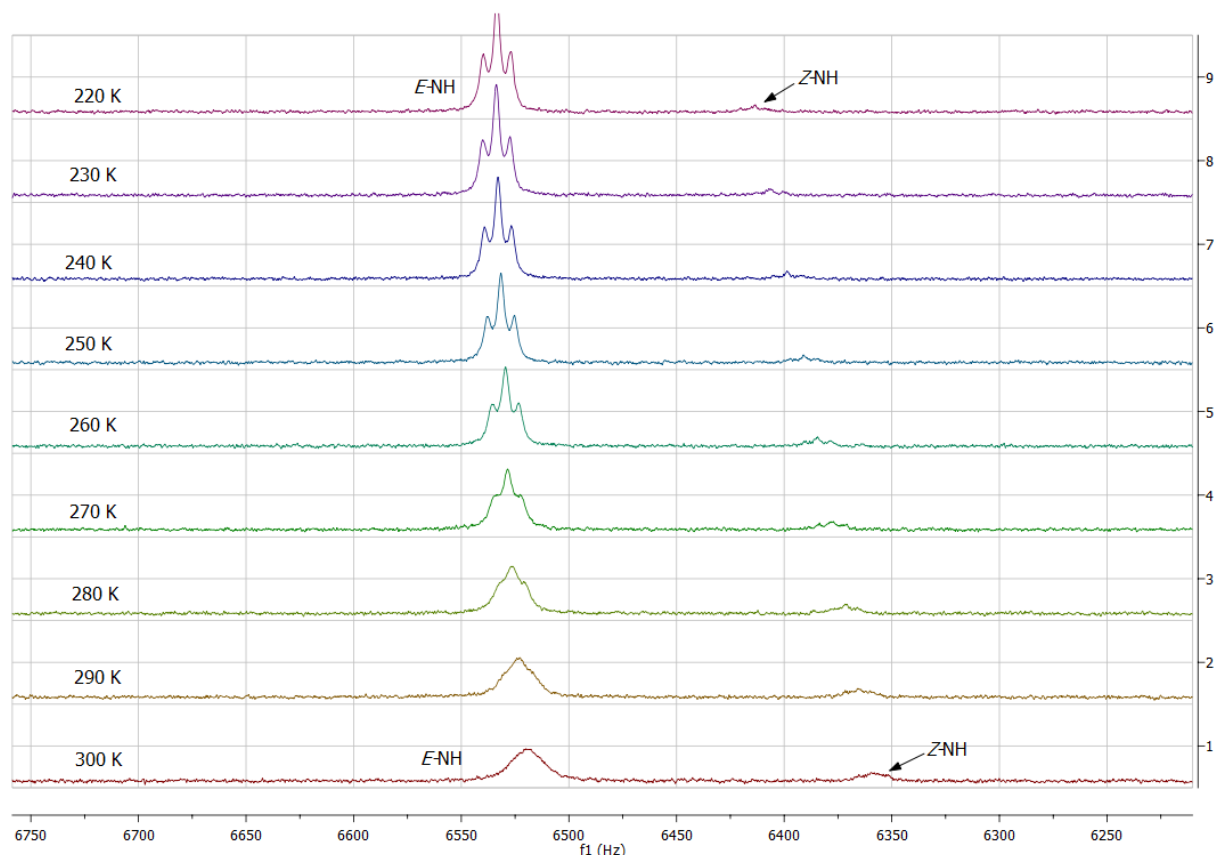
MS-ESI spectra for 2-ZnOAc.



2.1. Temperature-dependent 600 MHz ^1H NMR spectra of (*E/Z*)-2 in CDCl_3 .

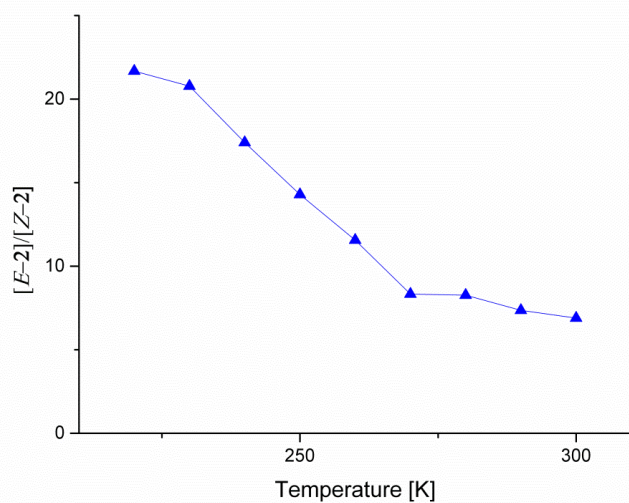


2.2. Partial temperature-dependent ^1H NMR spectra for *E*-NH, *Z*-NH of (pS/pR)-2 soluble in CD_3Cl .

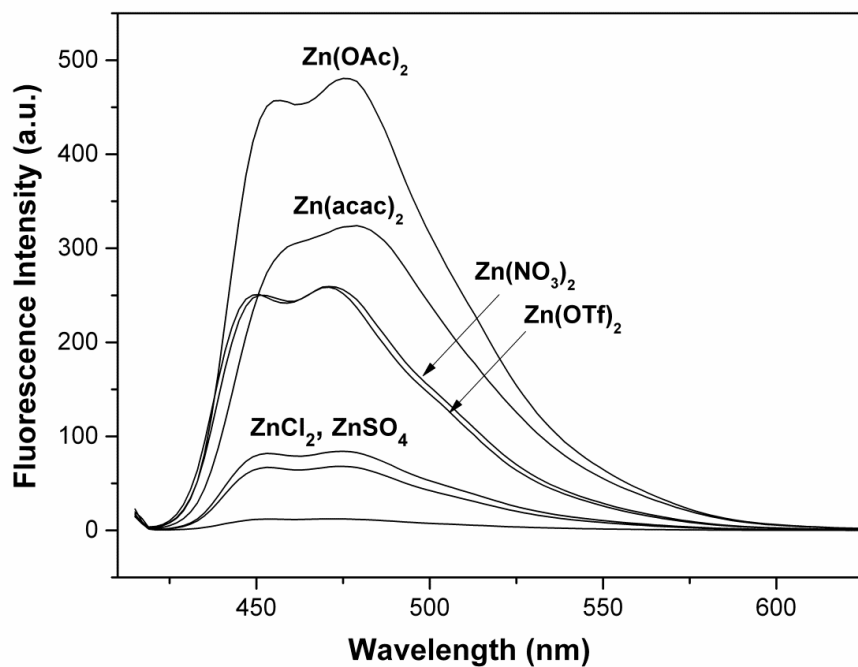


2.3 [*E*-2]/[*Z*-2] temperature dependence.

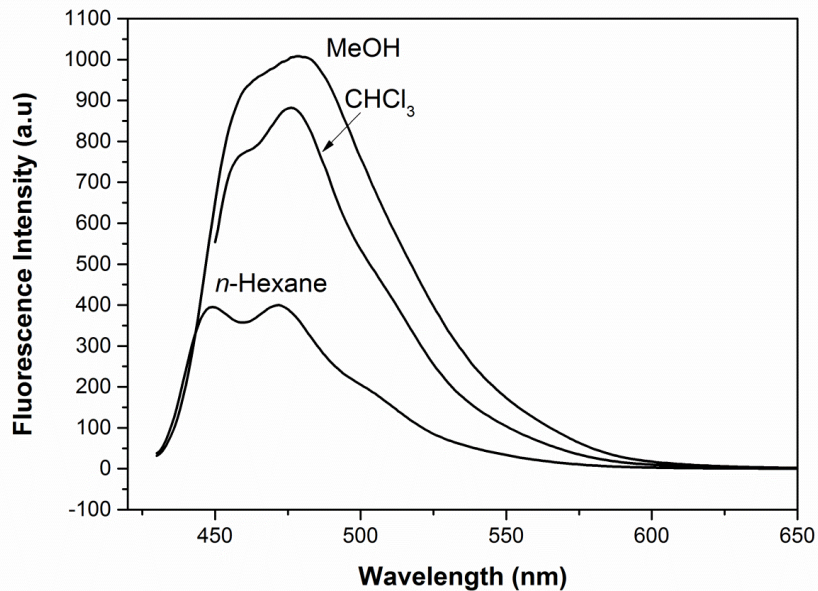
$[E\text{-}2]/[Z\text{-}2]$ was determined according the populations of *E*-NH and *Z*-NH for (*pS/pR*)-**2** soluble in CD₃Cl (note that crystalline phase of (*pS/pR*)-**2** contains two water molecules per unit cell) .



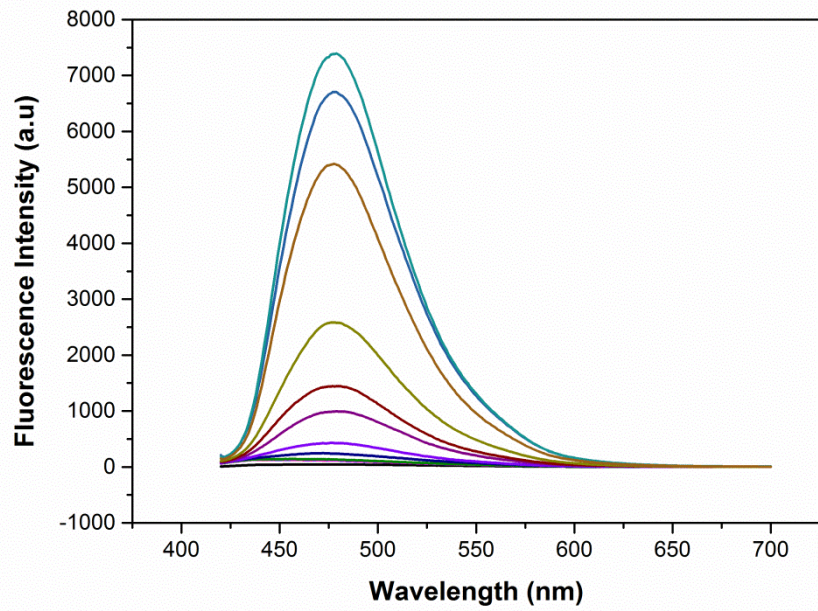
3.a) Fluorescence spectra of **2** (10 μ M) in CH₃CN with 1.equiv. of different zinc salts: Zn(acac)₂, Zn(OAc)₂, Zn(OTf)₂, Zn(NO₃)₂, ZnSO₄, and ZnCl₂ ($\lambda_{\text{ex}} = 410$ nm, voltage 400 V).



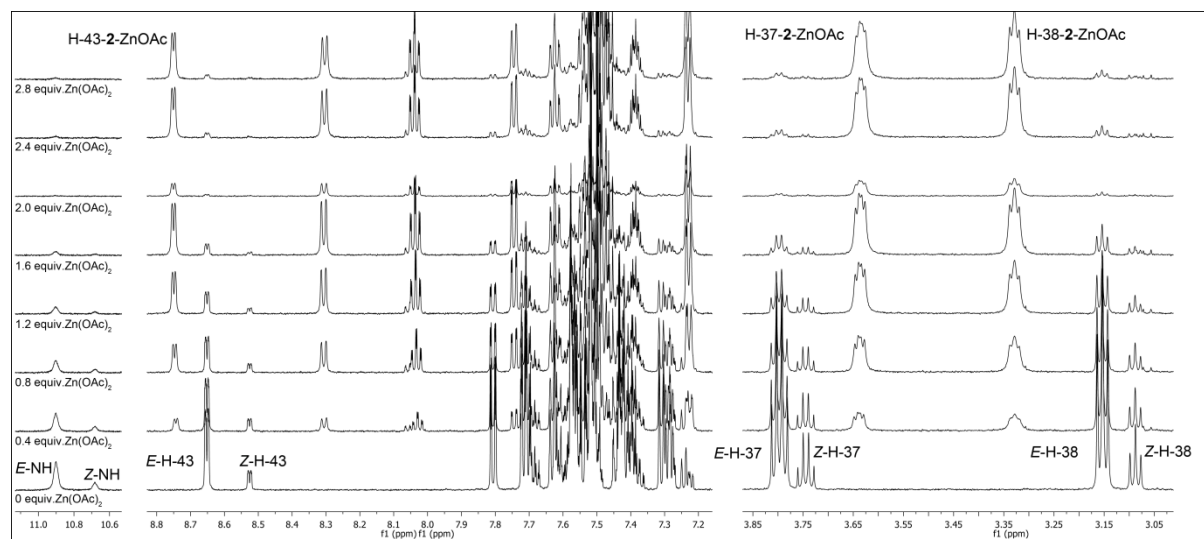
3.b) Fluorescence spectra of 2-ZnOAc in MeOH, CHCl₃, *n*-Hexane ($\lambda_{\text{ex}} = 410$ nm, voltage 400 V).



3.c) Fluorescence spectra of (*E/Z*)-2 (10 μ M) in acetonitrile/water mixture from 50% to 70% water fraction, ($\lambda_{\text{ex}} = 410$ nm, voltage 700 V).

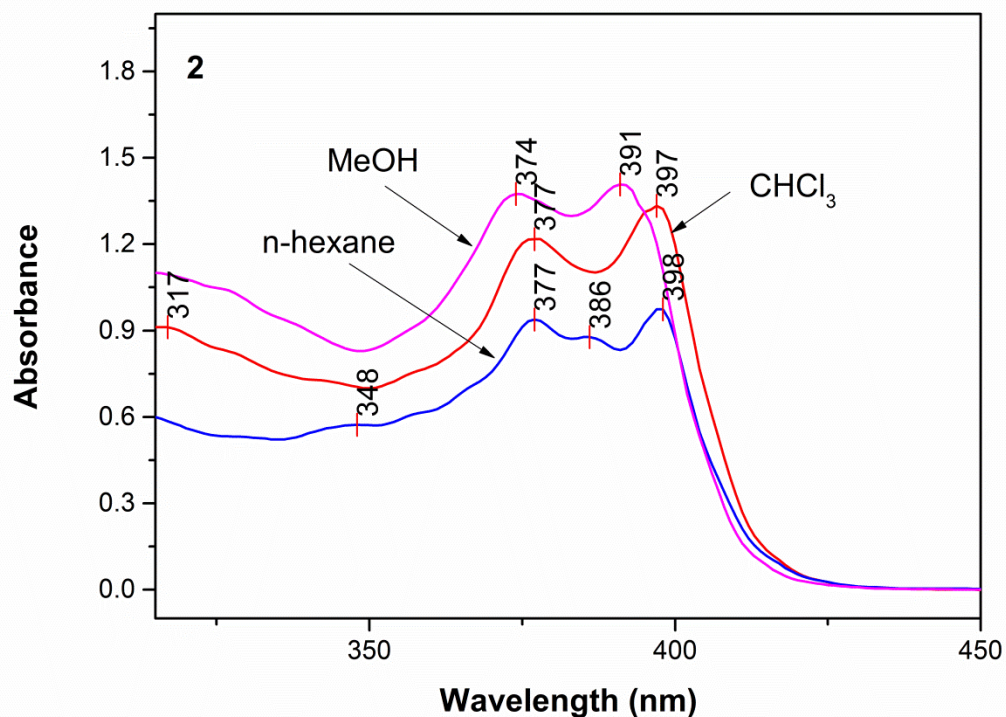


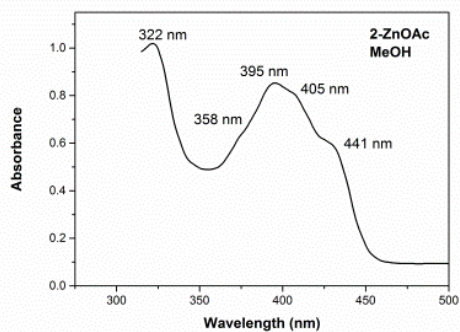
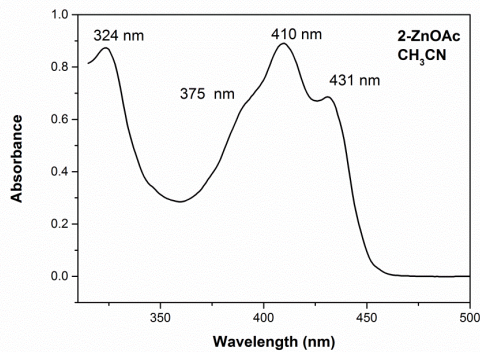
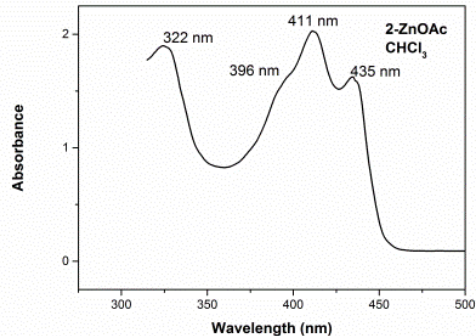
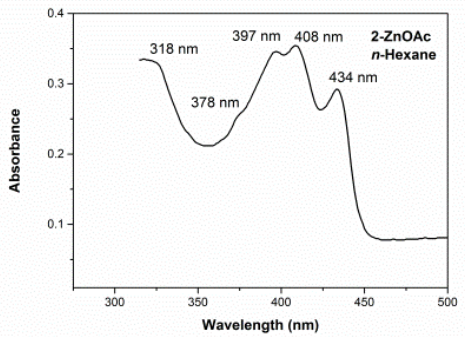
4. ^1H NMR spectra (600 MHz) of (*E/Z*)-2 (5 mM) upon titration with Zn(OAc)_2 in CD_3CN .



5. UV-VIS data.

- a) Absorption spectra of **2** in *n*-Hexane, CHCl_3 , MeOH, and **2**- ZnOAc in *n*-Hexane, CHCl_3 , CH_3CN , and MeOH.





- b) Determining associating constant from UV-VIS titration (P. Thordason, *Chem. Soc. Rev.*, 2011, **40**, 1305; P. Thordason, *Chem. Soc. Rev.*, 2011, **40**, 5922).

Association constant was estimated by fitting UV-Vis titration curve to the kinetic equation of 1:1 binding equilibria using non-linear regression method.

$$\hat{\mu} + A = \hat{\mu}_{\text{H}\ddot{\alpha}\text{G}}([HG]) = \hat{\mu}_{\text{H}\ddot{\alpha}\text{G}}^1 / 2 \left([G]_0 + [H]_0 + \frac{1}{K_a} \right) - \sqrt{\left([G]_0 + [H]_0 + \frac{1}{K_a} \right)^2 - 4[H]_0[G]_0}$$

Where general expression for equilibrium constant K_a is:

$$K_a = \frac{[HG]}{[H][G]}$$

$[G]_0$ – total concentration of zinc salt

$[H]_0$ - total concentration of ligand

Crystallographic data.

Table 1

Crystal data, intensity measurement conditions and structure refinement details.

Identification code	(pS)-2/(pR)-2*	(rac) -2**	2-ZnOAc
Crystal data			
Chemical formula	C ₃₀ H ₂₃ N ₅ O	C ₃₀ H ₂₃ N ₅ O	C ₃₂ H ₂₅ N ₅ O ₃ Zn
Solvent molecule	0.66 H ₂ O	none	CH ₃ CN
Mr	481.42	469.53	633.99
Wavelength (Å)	1.54184	1.54184	1.54184
Temperature (K)	120(2)	120(2)	120(2)
Crystal system	Monoclinic	Monoclinic	Monoclinic
Space group	P 2 ₁	C c	P 2 ₁ /n
Unit cell dimensions (Å, °)	<i>a</i> = 5.75094 (3) <i>b</i> = 17.80093 (8) <i>c</i> = 11.63481 (6) β = 98.7275 (5)	<i>a</i> = 12.65632 (9) <i>b</i> = 19.63117 (11) <i>c</i> = 19.20284 (11) β = 97.3451 (6)	<i>a</i> = 13.78516 (8) <i>b</i> = 14.11066 (8) <i>c</i> = 15.45815 (9) β = 101.3577 (5)
<i>V</i> (Å ³)	1177.289 (10)	4731.96 (5)	2948.00 (3)
<i>Z, Dx</i> (Mg/m ³)**	2, 1.358	8, 1.318	4, 1.428
μ (mm ⁻¹)	0.694	0.656	1.535
<i>F</i> (000)	505	1968	1312
Crystal size (mm)	0.35□0.30□0.20	0.53□0.50□0.40	0.50□0.30□0.20
Data collection			
θ Range (°)	8.10 – 76.93	4.18 – 76.80	3.93 – 76.87
Method	ω scans	ω scans	ω scans
<i>hkl</i> ranges	<i>h</i> : -6, 7; <i>k</i> : -22, 22; <i>l</i> : -14, 14	<i>h</i> : -15, 15; <i>k</i> : -24, 24; <i>l</i> : -24, 24	<i>h</i> : -17, 17; <i>k</i> : -17, 17; <i>l</i> : -19, 19
Reflections collected	46913	70316	60993
Reflections unique	4946	9907	6207
<i>R</i> (int)	0.0241	0.0252	0.0120
Reflections <i>I</i> > 2 σ (<i>I</i>)	4941	9840	6188
Completeness (%)	99.3	99.8	99.6
<i>T</i> _{min} , <i>T</i> _{max}	0.7933, 0.8737	0.7224, 0.7793	0.5140, 0.7288
Refinement			
Data/restraints/parameters	4946 / 8 / 361	9907 / 4 / 655	6207 / 3 / 406
Goodness-of-fit	1.043	1.036	1.091
<i>R</i> 1 [<i>I</i> > 2 σ (<i>I</i>)]	0.0366	0.0277	0.0390
<i>wR</i> 2 (all data)	0.0949	0.0725	0.1064
Extinction coefficient	none	none	none
Flack parameter	0.0(2)	0.09(11)	
Weighting scheme: <i>A, B</i>	0.0568, 0.3667	0.0462, 1.0346	0.0531, 3.0688

$\Delta\rho_{\max}$, $\Delta\rho_{\min}$ (e Å ⁻³)	0.405, -0.458	0.145, -0.177	1.041, -0.865
Rms (e Å ⁻³)	0.041	0.032	0.061

*(pS)-2/(pR)-2 with the ratio of (pS)-2 with C conformation to (pR)-2 with D conformation equals 0.828:0.172.

**(rac) - racemate containing equimolar (pR) and (pS) enantiomers of two symmetrically independent conformers A and B.

Diffractometer: Agilent SuperNova

Computer programs: CrysAlisPro [CrysAlisPro, Oxford Diffraction Ltd., Version 1.171.33.66], SIR92 [Altomare, A., Cascarano, G., Giacovazzo, C., Guagliardi, A., Burla, M. C., Polidori, G. & Camalli, M. (1994). J. Appl. Crystallogr. 27, 435] SHELXL97 [G.M. Sheldrick, Acta Crystallogr. A64 (2008) 112-122]; w = 1/[σ²(F_o²) + AP² + BP] where P = (F_o²+2F_c²)/3.

Table 2

Selected bond lengths (Å), valence angles (°), torsion angles (°) and dihedral angles (°) for ligand (pS)-**2**/(pR)-**2**, racemat (rac)-**2**, and Zn-complex **2**-ZnOAc·CH₃CN.

	(pS)- 2 /(pR)- 2 *	(rac)- 2 **	2 -ZnOAc	
	(pS)_C	(pR)_D	(pR)_A	(pR)_B
Bond lengths				
Zn(1)-O(3)				1.9541 (14)
Zn(1)-N(4)				1.9904 (14)
Zn(1)-N(30)				2.0225 (15)
Zn(1)-N(44)				2.0595 (16)
N(1)-C(2)	1.422 (2)		1.431 (1)	1.428 (1)
C(2)-O(2)	1.216(2)		1.220 (1)	1.220 (1)
C(2)-C(3)	1.460 (2)		1.454 (1)	1.460 (2)
C(3)-C(3a)	1.426 (2)		1.425 (2)	1.428 (2)
C(3a)-N(4)	1.314 (2)		1.311 (2)	1.310 (1)
N(4)-C(4a)	1.381 (2)		1.383 (1)	1.384 (1)
C(4a)-C(5)	1.416 (2)		1.404 (2)	1.409 (2)
C(5)-C(6)	1.381 (2)		1.376 (2)	1.379 (2)
C(6)-C(7)	1.406 (2)		1.403 (2)	1.401 (2)
C(7)-C(8)	1.374 (2)		1.378 (2)	1.376 (2)
C(8)-C(8a)	1.412 (2)		1.410 (2)	1.409 (2)
C(8a)-C(4a)	1.421 (2)		1.423 (2)	1.423 (2)
C(8a)-N(9)	1.388 (2)		1.392 (1)	1.389 (1)
N(9)-C(9a)	1.298 (2)		1.294 (1)	1.296 (1)
C(9a)-C(3a)	1.448 (2)		1.451 (1)	1.451 (1)
C(9a)-N(1)	1.379 (2)		1.387 (1)	1.387 (1)
C(3)-C(30)	1.396 (2)		1.394 (2)	1.394 (2)
C(30)-N(30)	1.328 (2)		1.327 (2)	1.330 (2)
N(30)-C(37)	1.465 (2)		1.468 (1)	1.467 (1)
C(37)-C(38)	1.497 (3)	1.336 (3)	1.517 (2)	1.512 (2)
C(38)-C(39)	1.468 (2)	1.500 (5)	1.515 (2)	1.507 (2)
C(39)-C(40)	1.390 (3) [#]	1.390 (5) [#]	1.394 (2)	1.387 (2)
C(40)-C(41)	1.390 (3)	1.390 (5)	1.382 (2)	1.384 (2)
C(41)-C(42)	1.390 (3)	1.390 (5)	1.374 (3)	1.384 (2)
C(42)-C(43)	1.390 (3)	1.390 (5)	1.378 (2)	1.369 (2)
				1.381 (3)

C(43)-N(44)	1.390 (3)	1.390 (5)	1.341 (2)	1.344 (2)	1.346 (3)
N(44)-C(39)	1.390 (3)	1.390 (5)	1.329 (2)	1.333 (2)	1.353 (2)
N(1)-C(11)	1.430 (2)		1.426 (1)	1.424 (1)	1.428 (2)
C(11)-C(12)	1.388 (2)		1.389 (1)	1.391 (2)	1.392 (3)
C(12)-C(13)	1.395 (2)		1.388 (1)	1.391 (2)	1.395 (3)
C(13)-C(14)	1.390 (2)		1.390 (2)	1.390 (2)	1.382 (3)
C(14)-C(15)	1.388 (3)		1.390 (2)	1.387 (2)	1.383 (3)
C(15)-C(16)	1.394 (2)		1.390 (2)	1.393 (2)	1.397 (3)
C(16)-C(11)	1.384 (2)		1.395 (2)	1.391 (2)	1.386 (3)
C(30)-C(31)	1.488 (2)		1.487 (2)	1.492 (2)	1.505 (2)
C(31)-C(32)	1.393 (2)		1.385 (2)	1.392 (2)	1.389 (3)
C(32)-C(33)	1.392 (3)		1.390 (2)	1.389 (2)	1.394 (3)
C(33)-C(34)	1.392 (3)		1.375 (2)	1.378 (2)	1.384 (4)
C(34)-C(35)	1.388 (3)		1.373 (2)	1.383 (2)	1.376 (4)
C(35)-C36)	1.385 (2)		1.387 (2)	1.393 (2)	1.396 (3)
C(36)-C(31)	1.395 (2)		1.387 (2)	1.392 (2)	1.394 (3)
C(45)-O(3)					1.283 (3)
C(45)-O(4)					1.231 (3)
C(45)-C(46)					1.509 (3)
C(47)-N(47)					1.137 (4)
C(47)-C(48)					1.454 (4)
Valence angles					
N(1)-C(2)-C(3)	106.4 (1)		106.4(1)	106.7 (1)	107.1(1)
O(2)-C(2)-C(3)	131.2 (1)		131.4 (1)	131.1 (1)	131.0(2)
C(2)-C(3)-C(3a)	107.3 (1)		107.5 (1)	107.3 (1)	106.9(2)
C(3)-C(3a)-N(4)	130.1 (1)		129.3 (1)	129.6 (1)	131.9(2)
C(3a)-N(4)-C(4a)	114.8 (1)		114.8 (1)	114.6 (1)	117.1(2)
C(8a)-N(9)-C(9a)	113.6 (1)		113.6 (1)	113.4 (1)	114.6(2)
N(9)-C(9a)-N(1)	126.9 (1)		127.7 (1)	127.0 (1)	126.6(2)
C(9a)-N(1)-C(2)	110.5 (1)		110.5 (1)	110.2 (1)	109.9(1)
N(1)-C(2)-O(2)	122.4 (2)		122.2 (1)	122.4 (1)	121.9(2)
O(2)-C(2)-C(3)	131.2 (2)		131.4 (1)	131.1 (1)	131.0(2)
C(2)-C(3)-C(30)	126.8 (2)		126.9 (1)	125.8 (1)	125.6(2)
C(3)-C(30)-N(30)	118.5 (2)		118.7 (1)	120.3 (1)	120.4(2)
C(30)-N(30)-C(37)	127.3 (1)		126.1 (1)	126.5 (1)	119.7(2)
N(30)-C(37)-C(38)	110.3 (1)	124.6 (2)	109.7 (1)	110.9 (1)	110.9(1)
C(37)-C(38)-C(39)	113.1 (2)	116.9 (2)	113.7 (1)	113.8 (1)	112.4(2)
C(38)-C(39)-N(44)	117.8 (1)	112.2 (5)	116.4 (1)	117.0 (1)	117.1(2)
C(39)-N(44)-C(43)	120.0 (2) [#]	120.0 (2) [#]	118.3(1)	117.8 (1)	119.2(2)
Torsion angles					

C(2)C(3)C(30)N(30)	168.0 (2)		178.9 (1)	-169.6 (1)	-176.7 (2)
C(3)C(30)N(30)C(37)	173.2 (2)		178.5 (1)	-170.9 (1)	-177.6 (2)
C(30)N(30)C(37)C(38)	-165.5 (2)	130.7 (2)	157.7 (1)	115.9 (1)	175.7 (2)
N(30)C(37)C(38)C(39)	-60.3 (2)	25.6 (4)	64.5 (1)	63.6 (1)	-66.7 (2)
C(37)C(38)C(39)N(44)	-67.7 (2)	31.8 (4)	31.1 (2)	10.9 (2)	68.9 (2)
C(38)C(39)N(44)C(43)	176.3 (2)	174.0 (2)	177.9 (1)	177.6 (1)	-176.9 (2)
C(2)C(3)C(30)C(31)	15.2 (3)		-1.0 (2)	10.2 (2)	4.6 (3)
C(3)C(30)C(31)C(32)	-54.8 (2)		-105.1 (1)	65.0 (2)	-75.0 (2)
C(2)N(1)C(11)C(12)	122.2 (2)		134.7 (2)	46.5 (2)	133.4 (2)
<i>Dihedral angles</i>					
N1^C9a - C11^C16	57.01 (3)		45.76 (3)	49.43 (3)	46.08 (6)
N1^C9a - C31^C36	62.27 (4)		76.13 (4)	70.85 (2)	73.67 (5)
N1^C9a - C39^N44	81.33 (5)	67.5 (2)	78.88 (3)	73.04 (6)	62.01 (5)

*(pS)-2/(pR)-2 with the ratio of (pS)-2 with C conformation to (pR)-2 with D conformation equals 0.828:0.172.

**(rac) - racemate containing equimolar (pR) and (pS) enantiomers of two symmetrically independent conformers A and B.

Because of the conformational disorder in the crystal structure of *(pS)-2/(pR)-2 for pyridine ring constrains according SHELXL97 where imposed assuming all bonds between non-hydrogen atoms as 1.390 Å and all endocyclic valence angles as 120 °.

Table 3

Hydrogen bond geometry and selected weak interactions (\AA , $^\circ$).

	D-H	H...A	D...A	$\angle \text{DHA}$
(pS)-2/(pR)-2				
N(30)-H(30)...N(4)	0.86(1)	2.12(2)	2.859(2)	143 (2)
N(30)-H(30)...N(44D)	0.86(1)	2.25(2)	2.716(3)	114(2)
O(45)-H(451)...O(2)	0.91	1.98	2.809(2)	151
O(45)-H(452)...N(44C) (-x+1, y+1/2, -z+1)	0.95	2.14	2.969(1)	144
C(16)-H(16)...N(9)	1.01	2.47(2)	3.476(2)	175
C(42A)-H(42C)...N(9)	0.95	2.51(2)	3.393(2)	154
Cg1...Cg3 (x+1, y, z) **			3.527(2)	
$\pi-\pi$ (x+1, y, z)***			3.406(2)	
(rac)-2				
N(30A)-H(30A)...N(44A)	0.89(1)	2.05(2)	2.811(1)	142(1)
N(30B)-H(30B)...N(4B) *	0.90(1)	2.22(2)	2.908(1)	134(1)
N(30B)-H(30B)...N(44B) *	0.90(1)	2.42(2)	2.939(2)	117(1)
C(43B)-H(43B)...Cg4(A) **	0.95	2.5	3.492	162
O(2A)...Cg5(A) **			3.492(2)	
O(2B)...Cg5(B) **			3.452(2)	
Cg2(A)...Cg3(B) **			3.397(2)	
Cg3(A)...Cg1(B) **			3.458(2)	
Cg2(A)...Cg2(B) **			3.493(2)	
Cg1(A)...Cg3(B) **			3.563 2)	
$\pi(\text{A})-\pi(\text{B})$ ***			3.507 (2)	
2-ZnOAc.CH₃CN				
C(48)-H(481)...O(4) (x, y, z-1)	0.98(2)	2.31(3)	3.197(4)	151(3)
C(38)-H(38B)...O(2) (-x+1/2, y-1/2, -z+3/2)	0.99	2.42	3.288(2)	147
C(48)-H(482)...N(47) (-x+1, -y, -z)	0.99	2.69	3.557	146
N(47)...Cg6			3.640 (3)	
Cg2...Cg3 (-x+1, -y+1, -z+1) **			3.455 (3)	
$\pi-\pi$ (x+1, y, z)***			3.353 (3)	

*bifurcated hydrogen bond

**The ring gravity centres: Cg1 for N(1)C(2)C(3)C(3a)C(9a), Cg2 for C(3A)N(4)C(4a)C(8a)N(9)C(9a), Cg3 for C(4a)C(5)C(6)C(7)C(8)C(8a) ring, Cg4 for C(11)C(12)C(13)C(14)C(15)C(16), Cg5 for C(31)C(32)C(33)C(34)C(35)C(36) and Cg6 for C(39)C(40)C(41)C(42)C(43)N(44)

*** π system of N(1)C(2)C(3)C(3A)N(4)C(4a)C(5)C(6)C(7)C(8)C(8a)N(9)C(9a) moiety

Fig. 6.1.1 Asymmetric part of the unit cell of (*rac*)–2 containing two symmetrically independent molecules both with planar chirality (*pR*) but of different conformation A and B. The molecules are in edge to face fashion (J-aggregation) with the interlayer distance of 3.397(2) Å. Although the crystal structure is non-centrosymmetric the space group *Cc* determines the structure of racemate. The non-hydrogen atoms are represented as displacement ellipsoids at 50 % probability level.

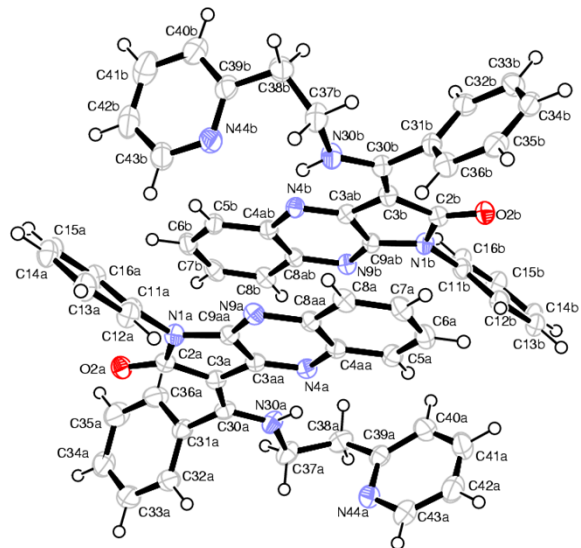


Fig. 6.1.2 (*rac*)–2: packing of the molecules viewed along [100]. The oxygen atoms O2 are marked for molecules A and B of planar chirality (*pR*). The oxygen atoms O2 of molecule with configuration (*pS*), related by glide plane ($x, -y, z+\frac{1}{2}$), are indicated by $(\underline{2})$. The structure is built of alternating layers along c-axis containing molecules with the same configuration. The non-hydrogen atoms are represented as displacement ellipsoids at 50 % probability level.

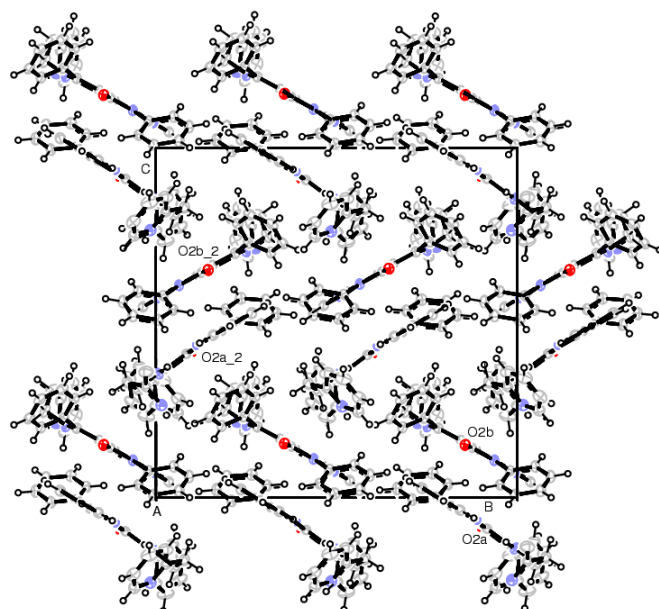


Fig. 6.1.3 Planar chirality (*pR*) of the molecules according the CIP rules (R.S. Cahn, C.K. Ingold, V. Prelog, *Experientia*, 1956, **12**, 81; R.S. Cahn, C.K. Ingold, V. Prelog, *Angew. Chem. Internat. Edit.*, 1966, **5**, 385) with conformation A and B forming dimer in the crystal structure of (rac)-**2** through strong π - π interaction. The non-hydrogen atoms are represented as displacement ellipsoids at 50 % probability level.

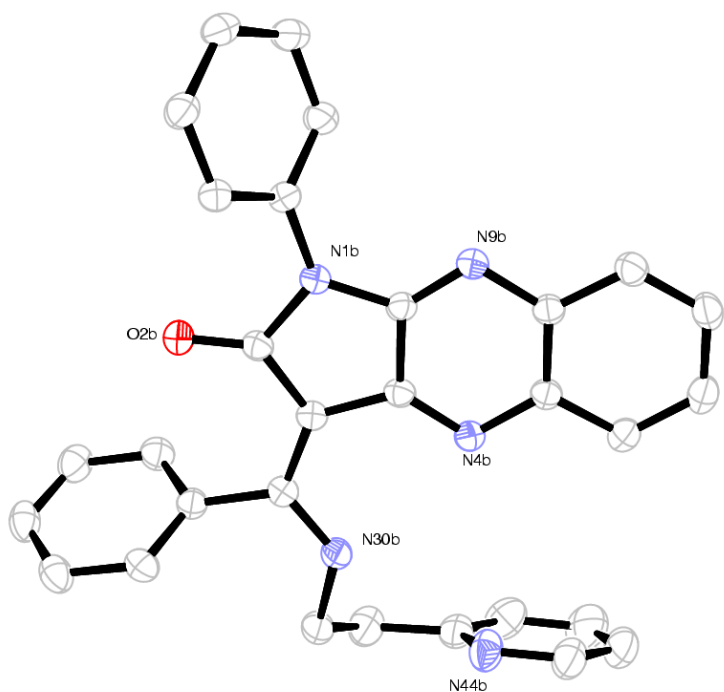
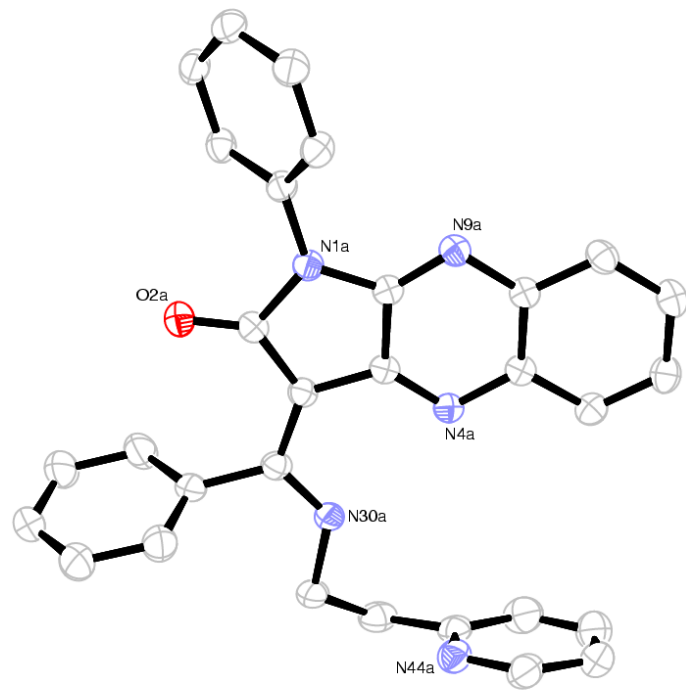


Fig. 6.1.4 Planar chirality (*pS*) of the molecules transformed by *c*-glide plane ($\perp 2$:
 $x, -y, z+\frac{1}{2}$) in the crystal structure of (*rac*)-**2** according the CIP rules (R.S. Cahn, C.K. Ingold,
V. Prelog, *Experientia*, 1956, **12**, 81; R.S. Cahn, C.K. Ingold, V. Prelog, *Angew. Chem. Internat. Edit.*, 1966, **5**, 385) with conformation A and B forming in the crystal structure
dimer through strong π - π interaction. The non-hydrogen atoms are represented as
displacement ellipsoids at 50 % probability level.

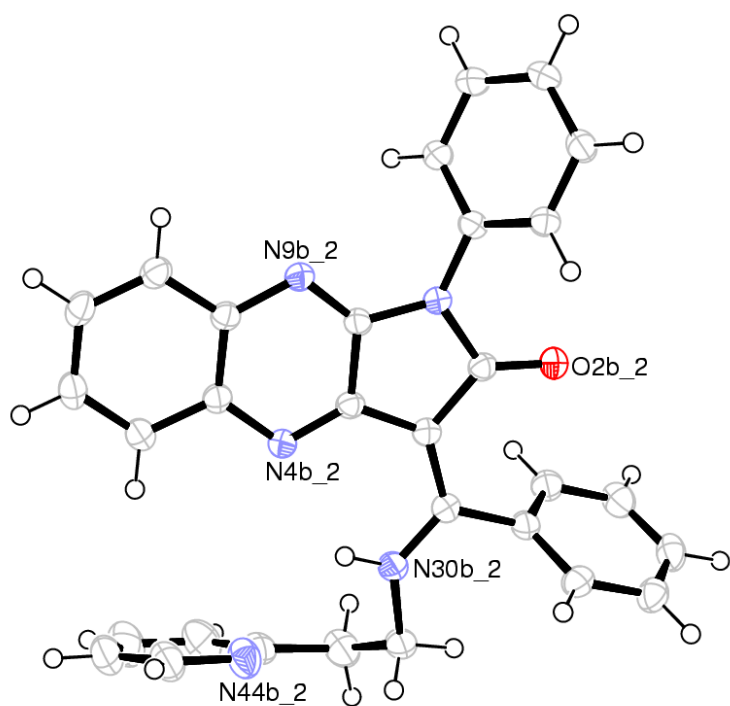
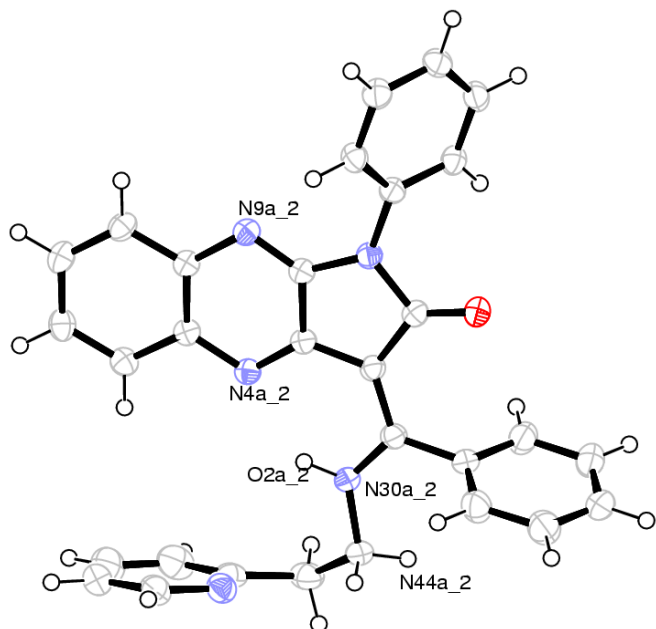


Fig. 6.2.1 Asymmetric part of the (pS)-2/(pR)-2 unit cell with the atom numbering scheme. The non-hydrogen atoms are represented as displacement ellipsoids at 50 % probability level.

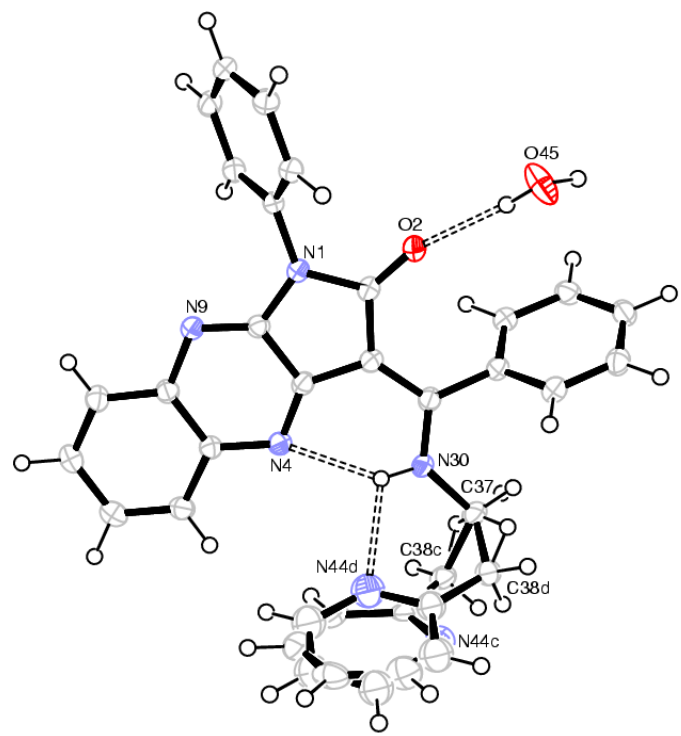


Fig. 6.2.2 (pS)-2/(pR)-2: The molecule of configuration (pS) and C-conformation (site occupancy factor of 0.828) is shown. The non-hydrogen atoms are represented as displacement ellipsoids at 50 % probability level.

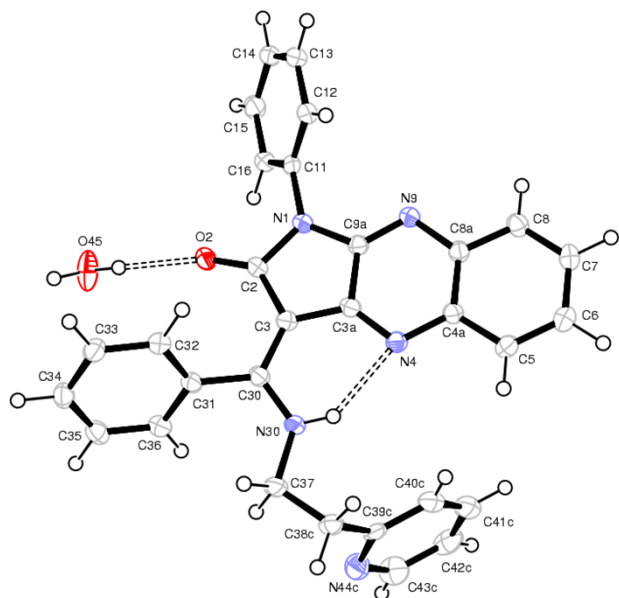


Fig. 6.2.3 (pS)-2/(pR)-2 unit cell with the atom numbering scheme: only (pR) molecule with D-conformation (site occupancy factor of 0.172) is shown. The non-hydrogen atoms are represented as displacement ellipsoids at 50 % probability level.

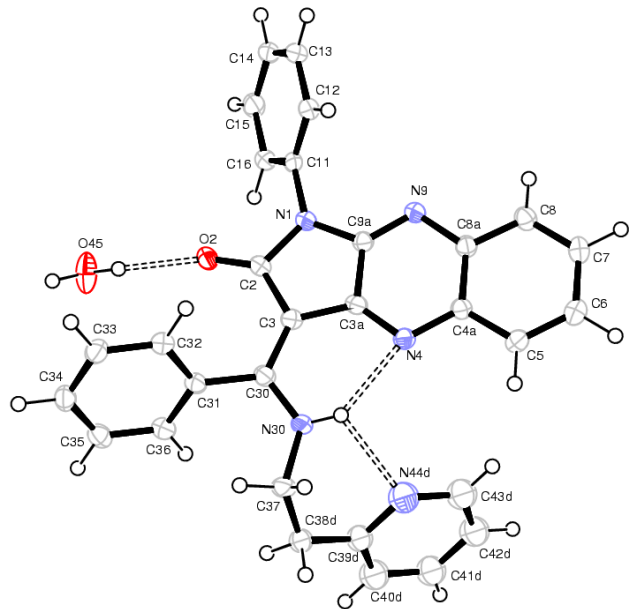


Fig. 6.2.4 (pS)-2/(pR)-2: packing of the (pS) molecules with C-conformation viewed along [100] is shown. For the first molecule nitrogen atom N44C, oxygen atoms O2 and O45 (water molecule) are marked. The non-hydrogen atoms are represented as displacement ellipsoids at 50 % probability level.

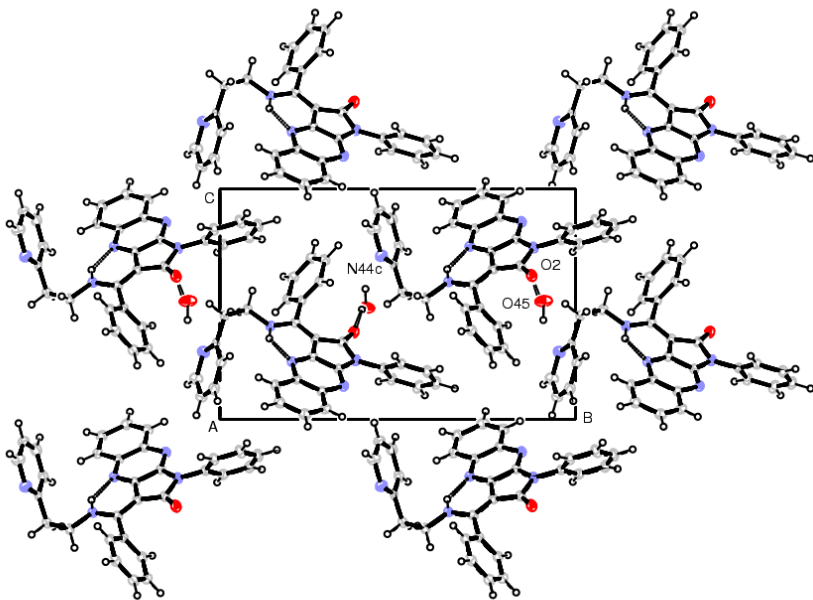


Fig. 6.3.1 Asymmetric part of the unit cell containing (R)-2-ZnOAc and acetonitrile molecules. Zinc atom is the stereogenic centre, however the crystal structure is centrosymmetric (racemate, space group $P\bar{2}_1/c$). Zn1 is coordinated to O3, N4, N30 and N44 atoms in the corners of distorted tetrahedron in distances 1.954(1), 1.990(1), 2.022(2) and 2.059(2) Å, respectively. The non-hydrogen atoms are represented as displacement ellipsoids at 50 % probability level.

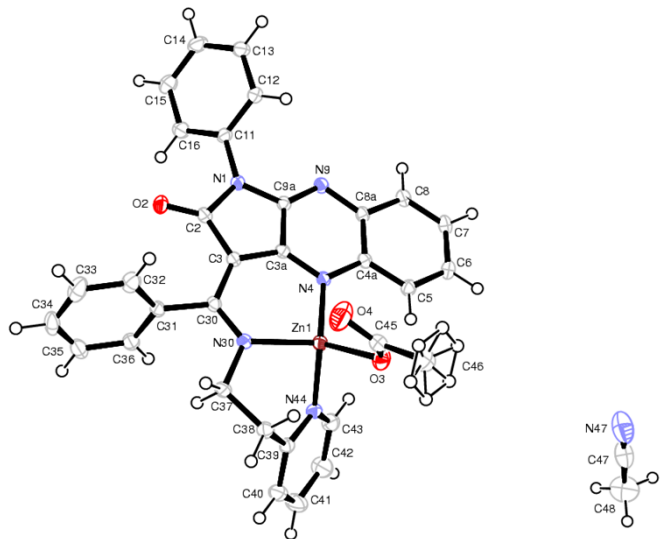


Fig. 6.3.2 Two molecules of 2-ZnOAc related by the centre of symmetry at $(\frac{1}{2}\frac{1}{2}\frac{1}{2})$ are 3.36(1) Å apart with the shortest distances between ring gravity centres being 3.455(1) Å for Cg2 (C3aN4C4aC8aN9C9a) and Cg3_3: (C4aC5C6C7C8C8a) at $(-x+1, -y+1, -z+1)$ and vice versa. The non-hydrogen atoms are represented as displacement ellipsoids at 50 % probability level.

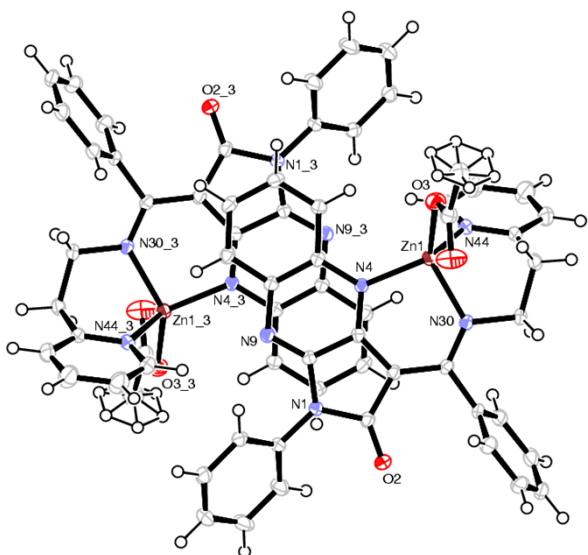


Fig. 6.3.3. $\text{2-ZnOAc}\cdot\text{CH}_3\text{CN}$: relation between solvent molecules and 2-ZnOAc complexes. Symbols: $_2$, $_3$, and $_4$ refer to symmetry operators $(-\text{x}+\frac{1}{2}, \text{y}-\frac{1}{2}, -\text{z}+\frac{1}{2})$, $(-\text{x}+1, -\text{y}, -\text{z})$, and $(\text{x}+\frac{1}{2}, -\text{y}+\frac{1}{2}, \text{z}-\frac{1}{2})$, respectively. The values of intermolecular distances are given in Table 3. The non-hydrogen atoms are represented as displacement ellipsoids at 50 % probability level.

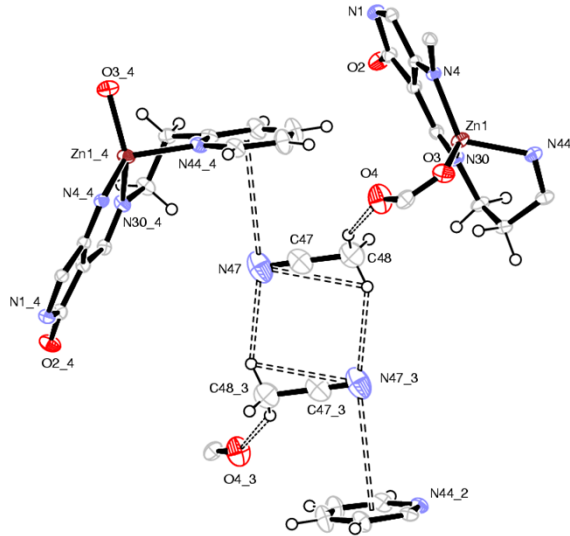


Fig.6.3.4. $\text{2-ZnOAc}\cdot\text{CH}_3\text{CN}$: packing of the molecules viewed along [001]. For the first molecule nitrogen atom N9 is marked. The non-hydrogen atoms are represented as displacement ellipsoids at 50 % probability level.

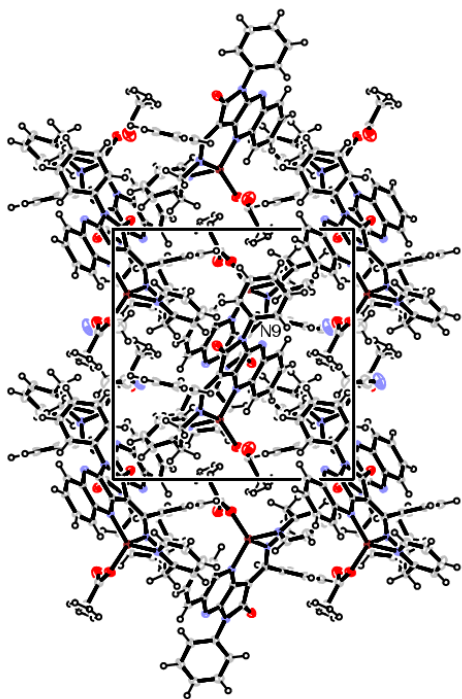
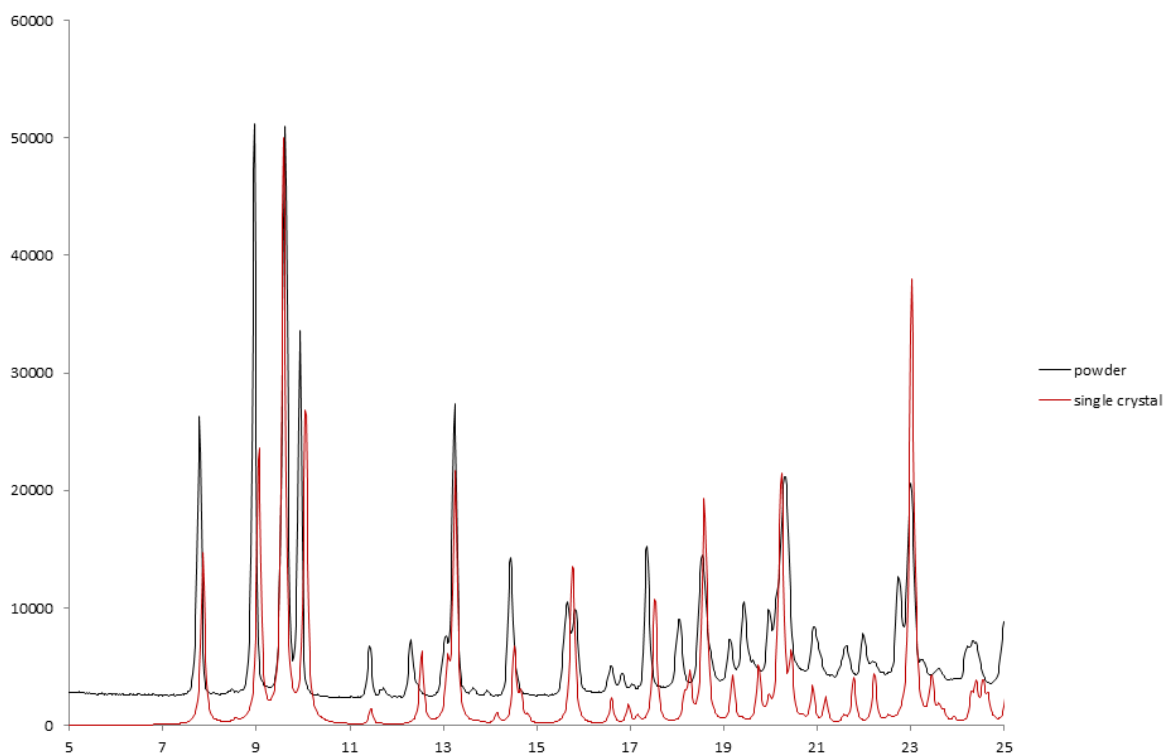


Figure 6.3.5. Experimental powder XRD pattern (black line) measured for **2-ZnOAc** on a PANalytical X’Pert PRO MPD diffractometer with a capillary spinning add-on using CuK α radiation ($\lambda = 1.54187 \text{ \AA}$). The pattern was collected at room temperature and compared with the reference powder pattern (red line) which was generated from the single crystal data at 120 K using Mercury 3.0 software. The diffraction maxima at room temperature fit well to those calculated at 120 K. Small differences and shift of peak position are caused by thermal expansion.



7. Topological analysis and *ab-initio* calculations.

Electron density and its topology analysis is extremely useful in modern materials chemistry. Utilization of Bader’s Quantum Theory of Atoms in Molecules (QTAIM) (R. F. W. Bader, *Atoms in molecules, A Quantum Theory*. New York: Oxford University Press, 2003; T. A. Keith (2010). AIMAll program (Version 10.11.24). aim.tkgristmill.com.) approach for the topological analysis of charge density enables characterization of any bond in the molecule in terms of so called critical points. Bond critical points (BCPs) are the extremes of the electron density in which the first derivative of $\rho(r)$ vanishes. BCPs are localized on so called bond paths, lines of the highest electron density linking two atoms. The value of second derivative of $\rho(r)$ - Laplacian at the BCP allows classification of interactions as shared-shell with density locally concentrated ($\nabla^2\rho(\mathbf{r}) < 0$, covalent bonds) or closed-shell with density locally depleted ($\nabla^2\rho(\mathbf{r}) > 0$, ionic bonds, weak interactions such as hydrogen bonds, van der Walls interactions). Ab initio calculations were performed for the isolated molecules of **2**-

ZnOAc at the DFT/B3LYP level of theory using B3LYP/6-31++G(d,p) basis set. The molecular geometry for “wave-function” calculations (Gaussian09, M. J. Frisch. et al., Gaussian 09. Revision A.1. Gaussian. Inc., Wallingford CT. 2009.) was taken from the crystal structure and modified assuming C-H bond lengths from neutron diffraction data (F. H. Allen and I. J. Bruno, *Acta Crystallogr. B.*, 2010, **66**, 380–6.). Potential intramolecular hydrogen bonds of C-H...O and C-H...N type do not fulfill Koch and Popelier criteria (U. Koch and P. L. A. Popelier, *J. Phys. Chem.*, 1995, **99**, 9747–9754.) for hydrogen bonding thus can be considered only as weak van der Waals interactions. Also the H...H distance 2.949 Å exceeds twice the van der Waals radius of the hydrogen atom (2.4 Å), thus cannot be considered as hydrogen-hydrogen bonding.

Table 4. Properties of the Bond Critical Points for the closed shell Zn-O and Z-N interactions: $\rho(\mathbf{r}) / \text{e}\text{\AA}^{-3}$ – charge density, Laplacian – $\nabla^2\rho(\mathbf{r}) / \text{e}\text{\AA}^{-5}$ and eigenvalues of Hessian – $\lambda_1, \lambda_2, \lambda_3 / \text{e}\text{\AA}^{-5}$. R_{ij} – internuclear separations (Å), d_1, d_2 – distance between BCPs and atom 1, 2 respectively (Å), $V(\mathbf{r}_{\text{CP}}) / \text{e}\text{\AA}^{-5}$, $G(\mathbf{r}_{\text{CP}}) / \text{e}\text{\AA}^{-5}$ local kinetic and local potential energy density, respectively.

	$\rho(\mathbf{r})$	$\nabla^2\rho(\mathbf{r})$	R_{ij}	d_1	d_2	$G(\mathbf{r}_{\text{CP}})$	$V(\mathbf{r}_{\text{CP}})$	$E(\mathbf{r}_{\text{CP}})$	$ V(\mathbf{r}_{\text{CP}}) / G(\mathbf{r}_{\text{CP}})$	$E(\mathbf{r}_{\text{CP}}) / r(\mathbf{r})$
Zn1-O3	0.090	0.434	1.954	0.943	1.011	0.125	-0.142	-0.017	1.133	-0.184
Zn1-N4	0.091	0.354	1.991	0.952	1.039	0.113	-0.137	-0.024	1.217	-0.268
Zn1-N30	0.086	0.317	2.022	0.964	1.058	0.102	-0.125	-0.023	1.224	-0.266
Zn1-N44	0.078	0.291	2.060	0.981	1.079	0.092	-0.111	-0.019	1.209	-0.248
C2-O2	0.417	-0.682	1.219	0.425	0.794	0.573	-1.316	-0.743	2.298	-1.783
C3-C2	0.278	-0.687	1.459	0.750	0.710	0.077	-0.325	-0.248	4.240	-0.892
C30-C3	0.287	-0.745	1.434	0.699	0.735	0.082	-0.350	-0.268	4.276	-0.933
N1-C2	0.282	-0.775	1.429	0.586	0.843	0.126	-0.445	-0.319	3.542	-1.131
C30-N30	0.361	-1.154	1.309	0.501	0.808	0.248	-0.785	-0.537	3.161	-1.485

Table 5. Atomic charges derived from QTAIM

Atom	$q(\Omega)$	Atom	$q(\Omega)$
Zn1	1.26	O3	-1.22
N30	-1.06	O4	-1.20
C30	0.55	N4	-1.08
C3	-0.06	N44	-1.04
C2	1.24	C3a	0.46
O2	-1.14	C9a	0.90